In silico pharmacophore study and structural optimization of Nafamostat yield potentially novel Transmembrane Protease Serine 2 (TMPRSS2) inhibitors which block the entry of SARS-CoV-2 virus into human cells

Bach X. Nguyen

Department of Chemistry, Graduate School of Science, Nagoya University, Chikusa-ku, Nagoya, Aichi 464-8602, Japan

Email: nguyen.bach.xuan@g.mbox.nagoya-u.ac.jp

Abstract

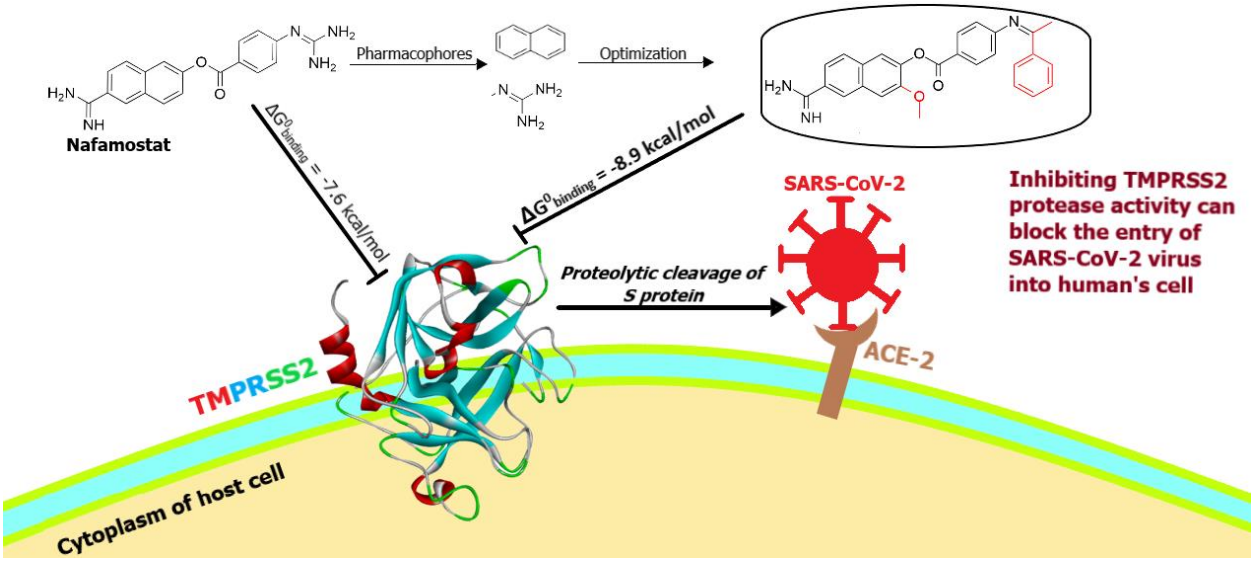

The past 6 months since December 2019 were marked by the COVID-19 pandemic caused from the Severe acute respiratory syndrome coronavirus 2 (SARS-CoV-2). Due to the urgent state worldwide, many efforts have been directed on repurposing approved drugs to facilitate the discovery of effective therapies. In this work, I employ molecular docking (*in silico*) as an approach to study the intermolecular interactions between Nafamostat mesylate – an approved anticoagulant drug, and transmembrane serine protease 2 (TMPRSS2) which is crucial for coronaviruses to enter host cells. Furthermore, structural optimization of Nafamostat is performed using pharmacophoric approach which indicates some small molecules as potentially effective TMPRSS2 inhibitors and pharmaceutical candidates for COVID-19 pandemic.

Keywords: SARS-CoV-2; molecular docking; Nafamostat; pharmacophore; drug optimization; TMPRSS2 inhibitors

Introduction

The 2019-nCoV acute respiratory disease caused from the SARS-CoV-2 virus originated from a seafood market in the city of Wuhan, Hobei Province, China [1].According to the Johns Hopkins Coronavirus Resource Center, a milestone of 4 million cases and more than 280,000 deaths have been reported worldwide as of the beginning of May. The United States remains the epicenter, accounting for approximately one third of all infected cases and more than 70000 deaths. There have been many attempts to accelerate the discovery of effectively therapeutic treatments such as vaccines [2], combination of antiviral drugs [3], and convalescent plasma therapy [4]. Meanwhile, repurposing of existing drugs is also an auspicious approach to provide urgent medicinal therapy for COVID-19 patients. Most of those drugs are repositioned to inhibit the entry of coronaviruses into human's cells [5].

SARS-CoV-2 particles utilize their spike (S) proteins located on the surface to enter human's cells [6]. These proteins consist of two functional subunits (S1 & S2) in which the surface S1 subunit containing the receptor binding domain(s) is responsible for the attachment of spike protein to the cellular receptor whereas the membrane-anchored S2 subunit regulates the fusion of the viral and host's membranes [6-9]. The serine protease anchored on the plasma membrane is reported to be essential for viral entry and spread in infectious host cells as it is involved in the protein priming of viral spike protein [6,9]. The infectious process of SARS-CoV-2 is initiated by the binding of viral S1 subunit to the cellular receptor followed by the priming of S protein by the host transmembrane serine protease 2 (TMPRSS2) [10]. The protease cleaves viral S protein at a specific site located right upstream of the fusion peptide which leads to the membrane fusion via irreversibly conformational changes [11,12]. This result is confirmed by various studies including cellular expression assays and responses to serine protease inhibitors [6]. Inhibiting the activities of TMPRSS2 can block the entry of SARS-CoV-2 virus into targeted human cells; thus, it potentially reduces the transmissibility and infectivity of the virus tremendously. Therefore, many efforts have been made to discover and ameliorate small molecules for TMPRSS2 inhibitors with the expectation of finding the most optimal antiviral drug(s) which can be potentially used for COVID-19 treatment.

Nafamostat mesylate (Fusan), a drug which was developed in Japan as treatments for acute pancreatitis [13] and other diseases [14], has been reported to be a potential inhibitor of SARS-CoV-2 infection. In comparison with Camostat mesylate (Foypan) – a recently identified inhibitor of the viral infection, Nafamostat can exhibit its inhibitory activity at a concentration less than one-tenth that of the former one [15]. According to a study published in 2016, it was shown that Nafamostat specifically interfered with MERS-S-mediated membrane fusion, most likely by inhibiting proteolytic activity of TMPRSS2 [16]. Despite its great prospect, how this drug interacts with the target protein is insufficiently researched. In this work, pharmacophores of Nafamostat as well as its interactions with the protease are studied using

molecular docking. Furthermore, I also performed structural optimization to increase the pharmacodynamic properties of the original molecule.

After performing molecular docking between Nafamostat and TMPRSS2, I have hypothesized the essential interactions and the ligand's pharmacophores by manipulating its structure in such a manner that for each manipulation, one specific interaction is weaken. Based on these results, the original drug molecule is then optimized by elevating the essential interactions between the pharmacophores and the protease. Nine optimally novel molecules are finally generated with the decreases of binding energy fall in the range of 0.5 to 1.3 kcal/mol with respect to Nafamostat.

Methods

Docking simulations of Nafamostat and its designed analogues to the homology model of TMPRSS2 [17] were performed using AutoDock Vina [18]. The homology model of TMPRSS2 (PDB template 5CE1) [17] was used as a rigid acceptor for the docking studies. Initial structures of Nafamostat and its analogues were determined by MM2 energy minimization before performing docking simulations. Nine conformations were generated for each drug candidate, and docked conformations whose binding cavities near the catalytic triad [His, Asp, Ser] occupied by the drug candidates were selected as possible conformations [17]. These results were visualized by using Discovery Studio Visualizer (BIOVIA).

Results and Discussion

Intermolecular interactions between Nafamostat and TMPRSS2

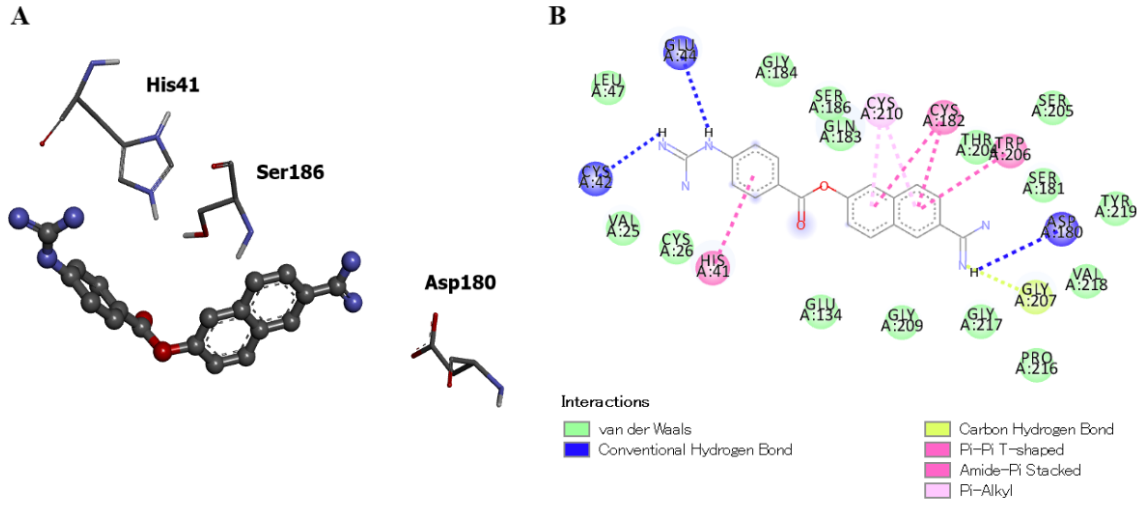

Figure 1. Structure and the interactions between Nafamostat and 5CE1 resulted from molecular docking
(A) Conformation of Nafamostat (Stick and ball) and the catalytic triad residues [His, Asp, Ser] (Stick)
(B) 2D diagram of TMPRSS2-Nafamostat interactions and the amino acid residues involved in the binding pocket.

The binding site is located near the TMPRSS2 catalytic triad comprising His, Asp, and Ser residues (Figure 1A) [17]. Binding energy of the docking model between Nafamostat and protein template 5CE1 is -7.6 kcal/mol. From the resulting model (Figure 1B), two conventional hydrogen bonds are formed between guanidine group and two amino acid residues (Cys42 and Glu44). Amidine core interacts with the protease via a conventional hydrogen bond with Asp180 and a carbon hydrogen bond with Gly207. As for phenyl group, there exists a π- π T-shaped interaction with the imidazolyl moiety of His41. Amide – π stacked interactions are formed between naphthalene group and two other amino acid residues (Cys182 and Trp206). Furthermore, π-alkyl interactions are found between naphthalene core and Cys210 residue. According to this docking model, the pharmacophores of Nafamostat can be preliminarily concluded to contain amidine, guanidine, phenyl and naphthalene moieties (Figure 1B).

Essential pharmacophores are validated by structural modifications of Nafamostat

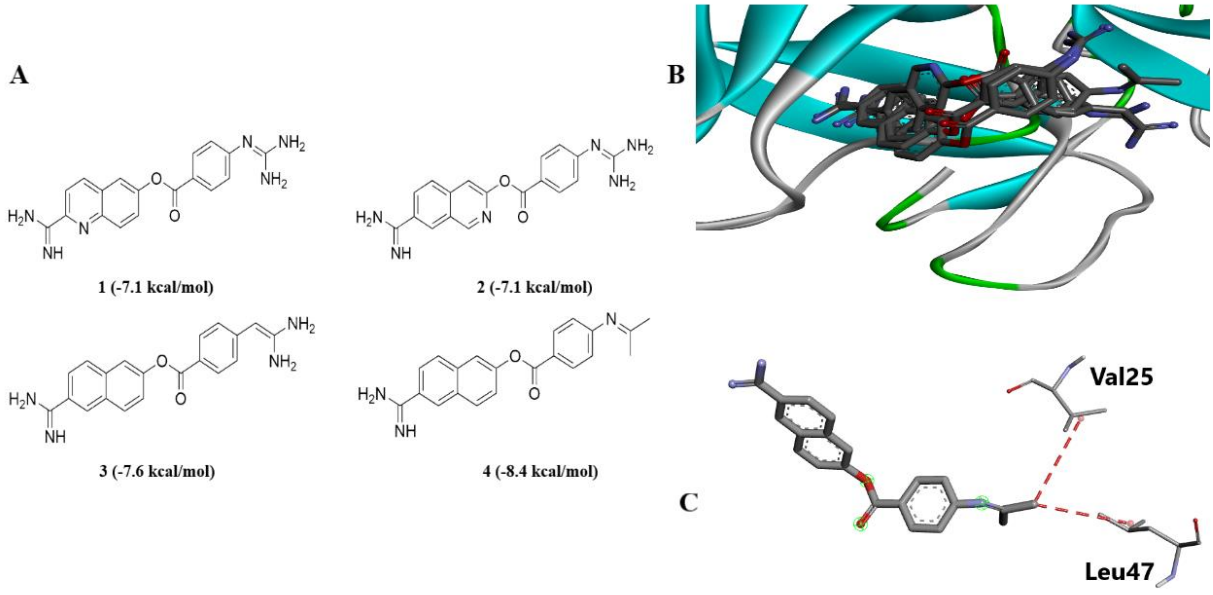

Figure 2. Pharmacophoric study by modifying molecular structure of Nafamostat (A) Modified molecules with their corresponding binding energies in the bracket (B) Representation of molecular poses of four modified molecules and Nafamostat in the protein's binding pocket (C) Representation of additionally hydrophobic interactions between methyl groups of compound **4** and two amino acid residues of TMPRSS2.

To further investigate the essential pharmacophores of Nafamostat, I designed four molecules (Figure 2A) and observed how these changes affect the binding affinity, taking the original molecule as reference. In addition to numerical affinity, I also evaluated these molecules' conformations with that of the original drug in the binding cavity (Figure 2B). Models with low binding energy values and highly overlapped poses with Nafamostat are considered the good ones and can be used to construct further hypotheses.

Because the amidine and phenyl group interact with two residues involved in the catalytic triad which are Asp180 and His41, respectively, they should be retained as original.

As for the naphthalene core, a nitrogen atom is introduced into one of the two aromatic rings to reduce the electronic density. Consequently, the ability of Nafamostat to form π interactions is deteriorated (compound **1** and **2**). Binding energies of both compounds have increased by 0.5 kcal/mol, which might imply that the naphthalene core is essential for the inhibitory activity of Nafamostat with TMPRSS2.

Next, I examined the essentiality of guanidine core by generating compound **3** and **4**. As for compound **3**, the sp^2 hybridized nitrogen atom is replaced by a carbon atom as I expected the former might exhibit hydrogen acceptor activity. However, the affinity remained unchanged, which indicates that this nitrogen atom is nonessential within the examining group. On the other hand, compound **4** was created by replacing two amino groups by two methyl groups as I anticipated this modification might interfere with their hydrogen bond formation abilities. Surprisingly, the model was significantly improved as the binding energy decreased to -8.4 kcal/mol. From this result, I supposed there might be hydrophobic residues of the protein that interact with the two methyl groups in compound **4**. Indeed, additional hydrophobic interactions are formed with Val25 and Leu47 residues in the binding pocket (Figure 2C).

Structural optimization of Nafamostat using previously pharmacophoric results

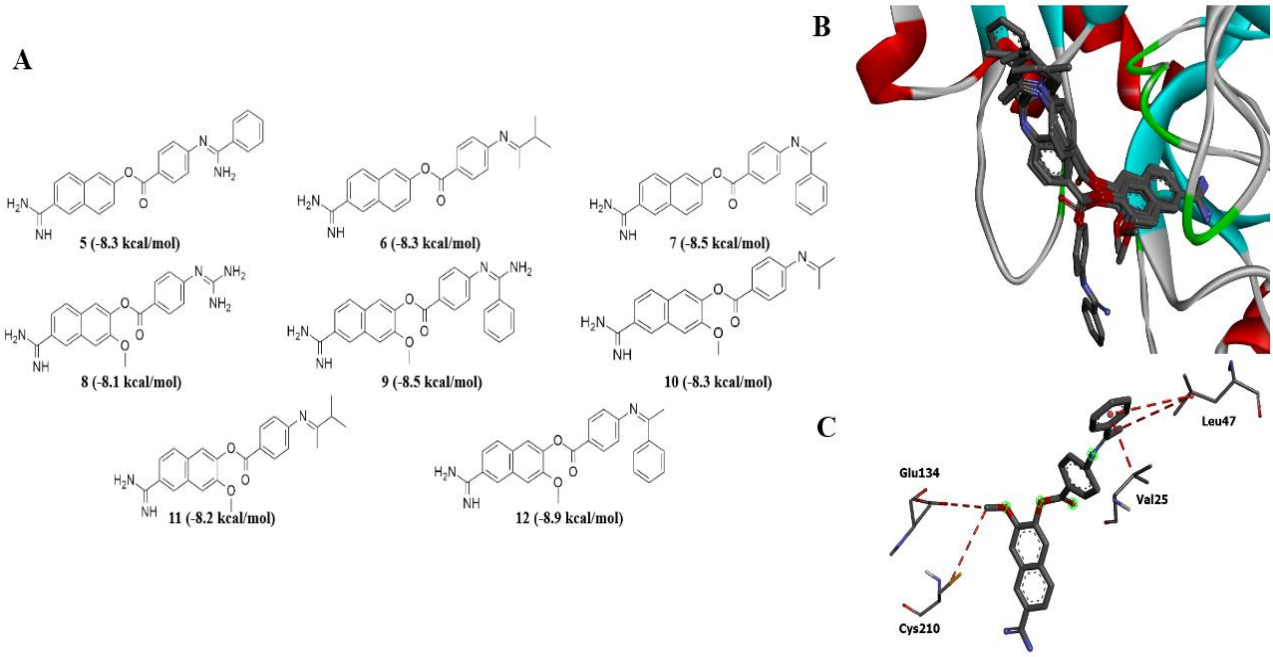

Figure 3. Structural optimization for Nafamostat (A) Optimized molecules with their corresponding binding energies in the bracket (B) Stick representation of molecular poses of eight novel molecules and Nafamostat in the protein's binding pocket (C) Representation of additional interactions between compound **12** and four amino acid residues of TMPRSS2.

With the previous results in hand, I performed structural optimization by modifying the two pharmacophores with the aim of reinforcing their interactions with the corresponding amino acid residues. Based on the information that the methyl groups of compound **4** form hydrophobic interactions with Val25 and Leu47 residues, I modified the guanidine core with various hydrophobic functional groups such as phenyl and isopropyl (compound **5-7**, Figure 3A). These novel compounds showed significantly ameliorated affinities; indeed, all three values of binding energy are declined at least 0.7 kcal/mol compared to that of Nafamostat. As for the naphthalene pharmacophore, I modified its structure by adding different electron donating groups such as methoxy (compound **8**, Figure 3A) so that the electronic density of the aromatic system is elevated (***S1***, Supplementary Information). Other compounds with the inclusion of methyl and isopropyl groups are also investigated (***S2***, Supplementary Information). The binding energy of compound **8** is diminished by 0.6 kcal/mol compared to the original drug molecule. Then, putting these two results together, I designed four novel molecules (compound **9-12**, Figure 3A) and examined their tendencies in binding energy. In general, they all exhibit significantly better affinity than Nafamostat with the binding energy values are in the range of -8.2 kcal/mol to -8.9 kcal/mol. In addition to numerical affinity, I also ensured that all the novel molecules are in the binding pocket and their molecular poses are relatively similar to that of Nafamostat (Figure 3B). From nine newly optimal compounds (including compound **4**), I decided to proceed further study of molecular interactions for compound **12** as it showed the best numerical affinity with TMPRSS2. In addition to the inherent interactions of Nafamostat, this novel compound shows extra intermolecular interactions with Val25, Leu47, Glu134, and Cys210 within the binding pocket. In more detail, phenyl and methyl group of the modified guanidine core hydrophobically interacts with Val25 and Leu47 whereas the additional methoxy group forms additional interactions with Glu134 and Cys210 (Figure 3C).

Conclusion

In the present study, I generated potential TMPRSS2 inhibitors by elevating the pharmacodynamical property of Nafamostat with TMPRSS2 using computational docking. Nine optimally novel molecules are finally generated with the decreases of binding energy fall in the range of 0.5 (compound **8**) to 1.3 kcal/mol (compound **12**) with respect to the original anticoagulant drug. The molecular docking becomes an ideal method especially when most laboratories are closed due to the epidemic situation. Nonetheless, further experimental studies should be carried out to examine the novel molecules' therapeutic effects. My finding adds some information that might enrich the library of serine protease inhibitors and lead to pharmaceutical candidates for COVID-19 pandemic.

Acknowledgements

I would like to thank Dr. S. Ariyasu (Nagoya University) for the great support with molecular docking. I would also thank Ms. P. Pham (Nagoya University) for the precious comments on the manuscript.

Declaration of interests

There are no competing financial interests.

References

[1]: Wu, D., Wu, T., Liu, Q., and Yang, Z. (2020). The SARS-CoV-2 outbreak: What we know: *International Journal of Infectious Diseases*, v. 94, p. 44–48.
https://doi.org/10.1016/j.ijid.2020.03.004

[2]: Chen, W.-H., Strych, U., Hotez, P. J., & Bottazzi, M. E. (2020). The SARS-CoV-2 Vaccine Pipeline: an Overview. *Current Tropical Medicine Reports*.
https://doi.org/10.1007/s40475-020-00201-6

[3]: Hung, I. F.-N., Lung, K.-C., Tso, E. Y.-K., Liu, R., Chung, T. W.-H., et al. (2020). Triple combination of interferon beta-1b, lopinavir–ritonavir, and ribavirin in the treatment of patients admitted to hospital with COVID-19: an open-label, randomized, phase 2 trial: *The Lancet*.
https://doi.org/10.1016/s0140-6736(20)31042-4

[4]: Duan, K., Liu, B., Li, C., Zhang, H., Yu, T., et al. (2020). Effectiveness of convalescent plasma therapy in severe COVID-19 patients. *Proceedings of the National Academy of Sciences*, 117(17), 9490–9496.
https://doi.org/10.1073/pnas.2004168117

[5]: Guy, R. K., DiPaola, R. S., Romanelli, F., & Dutch, R. E. (2020). Rapid repurposing of drugs for COVID-19. *Science*, eabb9332.
https://doi.org/10.1126/science.abb9332

[6]: Hoffmann, M., Kleine-Weber, H., Schroeder, S., Krüger, N., Herrler, T., et al. (2020). SARS-CoV-2 Cell Entry Depends on ACE2 and TMPRSS2 and Is Blocked by a Clinically Proven Protease Inhibitor: *Cell*, v. 181, p. 271–280.e8.

[7]: Ou, X., Liu, Y., Lei, X., Li, P., Mi, D., et al. (2020). Characterization of spike glycoprotein of SARS-CoV-2 on virus entry and its immune cross-reactivity with SARS-CoV. *Nature Communications*, 11(1). https://doi.org/10.1038/s41467-020-15562-9.

[8]: Lan, J., Ge, J., Yu, J., Shan, S., Zhou, H., et al. (2020). Structure of the SARS-CoV-2 spike receptor-binding domain bound to the ACE2 receptor: *Nature*, v. 581, p. 215–220. https://doi.org/10.1038/s41586-020-2180-5

[9]: Madu, I. G., Roth, S. L., Belouzard, S., & Whittaker, G. R. (2009). Characterization of a Highly Conserved Domain within the Severe Acute Respiratory Syndrome Coronavirus Spike Protein S2 Domain with Characteristics of a Viral Fusion Peptide. *Journal of Virology*, 83(15), 7411–7421. https://doi.org/10.1128/jvi.00079-09

[10]: Shang, J., Wan, Y., Luo, C., Ye, G., Geng, Q., Auerbach, A., & Li, F. (2020). Cell entry mechanisms of SARS-CoV-2. *Proceedings of the National Academy of Sciences*, 202003138. https://doi.org/10.1073/pnas.2003138117

[11]: Belouzard, S., Chu, V. C., & Whittaker, G. R. (2009). Activation of the SARS coronavirus spike protein via sequential proteolytic cleavage at two distinct sites. *Proceedings of the National Academy of Sciences*, 106(14), 5871–5876. https://doi.org/10.1073/pnas.0809524106

[12]: Wang, Q., Qiu, Y., Li, J.-Y., Zhou, Z.-J., Liao, C.-H., & Ge, X.-Y. (2020). A Unique Protease Cleavage Site Predicted in the Spike Protein of the Novel Pneumonia Coronavirus (2019-nCoV) Potentially Related to Viral Transmissibility. *Virologica Sinica*. https://doi.org/10.1007/s12250-020-00212-7

[13]: Otsuki, M., Hirota, M., Arata, S., Koizumi, M., Kawa, S., et al, & Research Committee of Intractable Diseases of the Pancreas (2006). Consensus of primary care in acute pancreatitis in Japan. *World journal of gastroenterology*, 12(21), 3314–3323. https://doi.org/10.3748/wjg.v12.i21.3314

[14]: Choi, J.-Y., Kang, Y.-J., Jang, H. M., Jung, H.-Y., Cho, J.-H., Park, S.-H., Kim, Y.-L., & Kim, C.-D. (2015). Nafamostat Mesilate as an Anticoagulant During Continuous Renal Replacement Therapy in Patients With High Bleeding Risk. *Medicine*, 94(52), e2392. https://doi.org/10.1097/md.0000000000002392

[15]: Bittmann S, Luchter E, Weissenstein A, Villalon G, Moschüring-Alieva E. TMPRSS2- Inhibitors Play a Role in Cell Entry Mechanism of COVID-19: An insight into Camostat and Nafamostat. *J Regen Biol Med*. 2020;2(2):1-3. https://doi.org/10.37191/Mapsci-2582-385X-2(2)-022

[16]: Yamamoto, M., Matsuyama, S., Li, X., Takeda, M., Kawaguchi, Y., Inoue, J., & Matsuda, Z. (2016). Identification of Nafamostat as a Potent Inhibitor of Middle East Respiratory Syndrome Coronavirus S Protein-Mediated Membrane Fusion Using the Split-Protein-Based Cell-Cell Fusion Assay. *Antimicrobial Agents and Chemotherapy*, 60(11), 6532–6539. https://doi.org/10.1128/aac.01043-16

[17]: Rensi, S., B Altman, R., Liu, T., Lo, Y.-C., McInnes, G., derry, alex, and keys, alli. (2020). Homology Modeling of TMPRSS2 Yields Candidate Drugs That May Inhibit Entry of SARS-CoV-2 into Human Cells: *Preprint* at https://doi.org/10.26434/chemrxiv.12009582.v1 (2020).

[18]: Trott, O., & Olson, A. J. (2009). AutoDock Vina: Improving the speed and accuracy of docking with a new scoring function, efficient optimization, and multithreading. *Journal of Computational Chemistry*, v. 31, p. 455–461. https://doi.org/10.1002/jcc.21334